International Journal of Thermophysics, Vol. 27, No. 6, November 2006 (© 2006)
DOI: 10.1007/s10765-006-0132-4

Nanostructure of Clusters in Nafion Studied by DSC[1]

M. Iijima,[2,3] Y. Sasaki,[4] T. Osada,[2] K. Miyamoto,[4] and M. Nagai[4]

The nanostructure that consists of clusters and channels between the clusters in Nafion with absorbed water is studied by Differential Scanning Calorimeter (DSC) measurements with stepwise temperature programs. A cluster size distribution (CSD) is fitted reasonably by a log normal distribution function. The fitted CSD has a peak of approximately 4 nm in diameter. In comparison of the water content from gravimetry with that from the fitted CSD, at least three kinds of water states are found, two of which are freezable and non-freezable water in a cluster and another is the non-freezable water in a channel between the clusters. From the assumption of a simple cubic lattice model, the channel length L_{ch} between the clusters and the cross section S_{ch} of the channel can be estimated. Also, the degree of desulfonation in the terminal of the side chain by thermal degradation depends on the nanostructure consisting of the clusters and channels in Nafion with absorbed water. The channel length L_{ch} decreases monotonically with increasing water content. Essentially the channel cross sectionS_{ch} increases with increasing water content.

KEY WORDS: cluster size distribution; DSC; Nafion; nanostructure; polymer electrolyte fuel cell (PEFC); thermoporosimetry.

1. INTRODUCTION

The state-of-the-art polymer electrolyte fuel cell (PEFC) utilizes perfluorosulfonic acid polymer membranes as electrolytes. Nafion membranes

[1] Paper presented at the Seventeenth European Conference on Thermophysical Properties, September 5–8, 2005, Bratislava, Slovak Republic.

[2] Department of Physics, Faculty of Engineering, Musashi Institute of Technology, Tamadutsumi 1-28-1, Setagaya-ku, Tokyo 158-8557, Japan.
[3] To whom correspondence should be addressed. E-mail: iijima@ph.ns.musashi-tech.ac.jp
[4] Department of Environmental Energy Engineering, Faculty of Engineering, Musashi Institute of Technology, Tamadutsumi 1-28-1, Setagaya-ku, Tokyo 158-8557, Japan.

consist of a polytetrafluoroethylene (PTFE) backbone with side-chains terminated with a sulfonate group. In many ionomers, the ionic species are observed to aggregate and form hydrophilic domains that are distributed through a polymeric matrix. The two-phase structure of the perfluorocarbon ionomers is due to the molecular aggregation of hydrophilic ionic groups separated from hydrophobic fluorocarbon chains. For the perfluorosulfonated ionomer membranes, the water content inside membranes is balanced by the hydrophobicity of the perfluorinated polymer backbones and the hydrophilicity of the terminal sulfonic acid. In the presence of water, only the hydrophilic domain is hydrated to maintain the proton conductivity.

The nanostructure in Nafion with absorbed water consists of many water clusters with distributed sizes and water channels that reside between the water clusters [1–3]. The nanostructure affects strongly the transport of the oxonium ion and proton hopping. In the transport the ions must go through the water cluster and the channels in Nafion with absorbed water. The small clusters and the fine channels play also an important role in the proton conductivity and ion transport. It is important for the development of a new polymer electrolyte to estimate the water cluster size distribution (CSD) in Nafion with absorbed water. The fuel cell performance is influenced strongly by thermal degradation related to the SO_2 liberation process between 250 and 300°C and the desulfonation process between 290 and 400°C for Nafion [4]. It is also interesting to understand the nanostructure in the thermally degraded Nafion in comparison with that in an as received state.

Recently, thermoporosimetry from Differential Scanning Calorimeter (DSC) has been proposed for silica gel. A pore size distribution can be estimated by means of the depression of the melting point due to the increase of the interfacial energy between silica and water within the pores [5,6]. In this study we estimate the CSD in Nafion with absorbed water as received and in thermally degraded Nafion from thermoporosimetry by DSC. From the obtained CSD we analyze the nanostructure that is formed with the clusters and the channels in the Nafion with absorbed water. Through an understanding of the relation between the nanostructure and proton conductivity, it will be possible to improve fuel cell performance.

2. EXPERIMENTAL

Nafion117 membrane supplied from DuPont is used in this study. The equivalent weight (EW) and the thickness of the membrane are 1100 g/eq. and 0.18 mm, respectively. Nafion is soaked in pure water at

room temperature (RT) for various lengths of time in order to control the water content. The water content W_c in Nafion is defined as follows:

$$W_c = \frac{W_{up} - W_{dry}}{W_{dry}}, \tag{1}$$

where W_{up} is the mass of the Nafion with absorbed water and W_{dry} is the dry Nafion mass after keeping it *in vacuo* for a long time, i.e., for a week.

The DSC measurements are carried out with a DSC822^e differential scanning calorimeter from Mettler Toledo equipped with a cooling apparatus. Conventional DSC curves are obtained in the temperature range between 5 and -50°C with a scanning rate of 5°C·min^{-1}. The DSC curves are obtained by a stepwise temperature program for heating in the temperature range from -50 to 5°C from which the CSD is estimated. The stepwise temperature program consisted of the repetition of two parts; the isothermal part while holding the temperature for 5–30 min and successive heating by up to 3°C with a rate of 0.3°C·min^{-1}. A sample mass of about 4.6 mg is put into an aluminum pan and purged with nitrogen. The temperature and enthalpy are calibrated with indium as a standard. The thermally degraded samples are prepared from aging at 25, 150, and 300°C for 1 h in the DSC apparatus.

The relationship between the spherical cluster diameter d and the melting temperature T_m, the well-known Gibbs–Thomson or Gibbs–Duhem equation, is used to fit the result for Nafion with absorbed water in Ref. [7] as follows:

$$d = \frac{64.04}{0.12 - T_m} + 0.80. \tag{2}$$

The number of water clusters N_{clu} per unit volume of the membrane is evaluated by the following equation:

$$N_{clu} = \frac{\Delta h / \Delta H_m}{\rho_w \frac{4}{3}\pi \left(\frac{d}{2}\right)^3} \frac{1}{V_{Naf}}, \tag{3}$$

where Δh is the measured melting enthalpy of water, ΔH_m is the melting enthalpy per unit mass of water, ρ_w is the density of water, and V_{Naf} is the volume of Nafion. The obtained CSDs are fitted by a log normal distribution for estimation of the total cluster volume, and this is taken into account to estimate the non-freezable water in clusters that are too small.

3. RESULTS AND DISCUSSION

3.1. Melting and Freezing Behavior of Water Clusters by Conventional DSC Measurements

Figure 1(a) shows cooling curves for Nafion with absorbed water for various W_c obtained from conventional DSC measurements. The sharp peak at high temperature is obtained for pure water. All other peaks occur at lower temperatures than that of pure water. These exothermic peaks are due to crystallization of water in Nafion with absorbed water. The exothermic peaks shift to higher temperatures, and the peak height increases with an increase in the water content in Nafion [8]. The crystallization

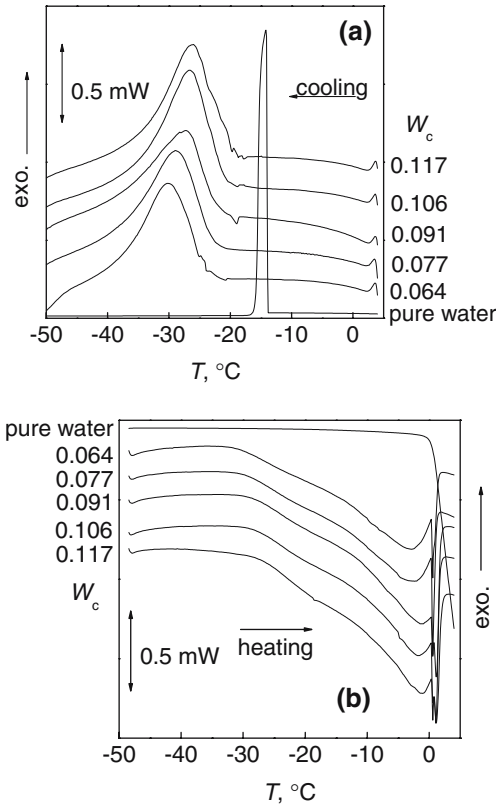

Fig. 1. DSC curves of (a) cooling and (b) heating for Nafion with absorbed water for various water content and pure water at a scanning rate of $5°C min^{-1}$.

behavior is characterized by a cluster size dependence of the melting temperature.

Figure 1(b) shows DSC heating curves for the same samples as shown in Fig. 1(a). The onset of the melting peak of pure water is shown in the top curve. The heating curves for water in Nafion have sharp peaks at about 0°C for the free water and asymmetrical broad peaks between −30 and 0°C due to the melting of water in the clusters. The broad peak temperature shifts to higher temperatures with increasing W_c.

3.2. Cluster Size Distribution (CSD)

Figure 2 shows the results of DSC measurements with a stepwise temperature program for Nafion with absorbed water for $W_c = 0.106$. The heat flow resulting from a pulse corresponds to heating between isothermal parts in the temperature program as shown in the inset. Therefore, the total enthalpies for the pulse heat flow include three contributions:

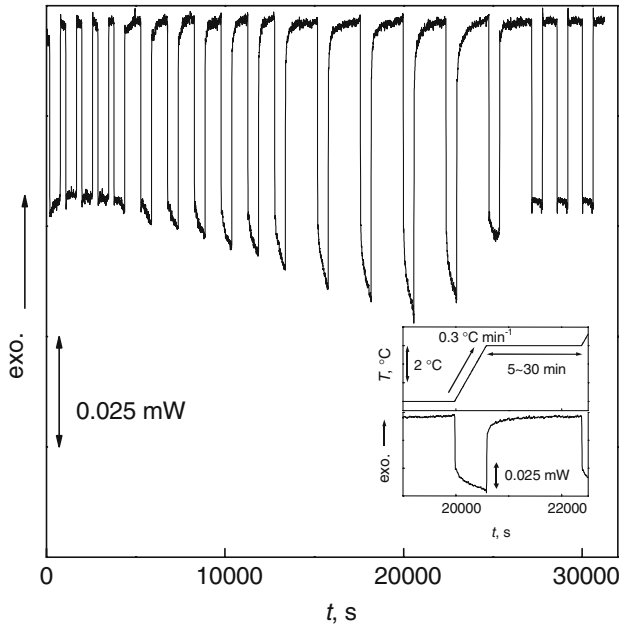

Fig. 2. DSC curve with a stepwise temperature program for Nafion with absorbed water (W_c = 0.106). Inset shows one step of the stepwise temperature program and the corresponding heat flow.

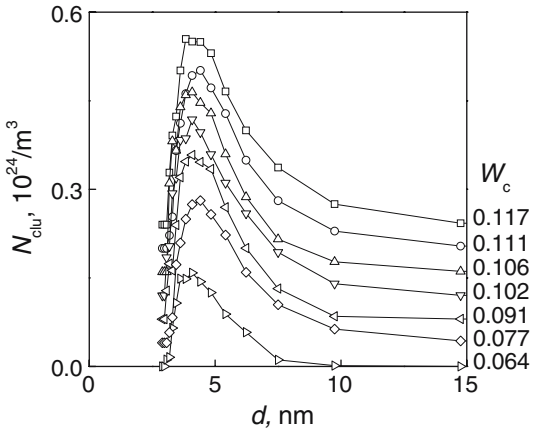

Fig. 3. CSD of Nafion with absorbed water for various water content. Each data point is shifted by 0.04 along the ordinate.

the specific heat of Nafion and molten water and the melting enthalpy of water by heating to 3°C.

From these results of the stepwise temperature program, we can calculate the CSD as spherical clusters for Nafion with absorbed water from Eqs. (2) and (3). The CSD drops sharply below 2 nm in diameter as shown in Fig. 3 because the water in clusters that are too small cannot crystallize. This behavior suggests the existence of a few percent of non-freezable water. We assume that the CSD can be fitted with a log normal distribution function as shown in the inset in Fig. 4. The fitted CSD for Nafion with absorbed water has a peak around 4 nm as shown in Fig. 4 and is consistent with SAXS results [1,8,9]. It is also found that both the peak position and height of the fitted CSD increase with increasing W_c. From the fitted CSD, we can evaluate the water content in the cluster as discussed later.

3.3. Water Uptake Process in Nafion

Three different cases of water content in Nafion with absorbed water are evaluated from the DSC results: W_c and the cluster water content and non-freezable water content from the fitted CSD. Figure 5 shows the contents of three kinds of water plotted as a function of soaking time in water. The amount of three kinds of water increases with increasing soaking time at the early stages and levels off after that. The non-freezable water content reaches saturation at an earlier soaking time than that of

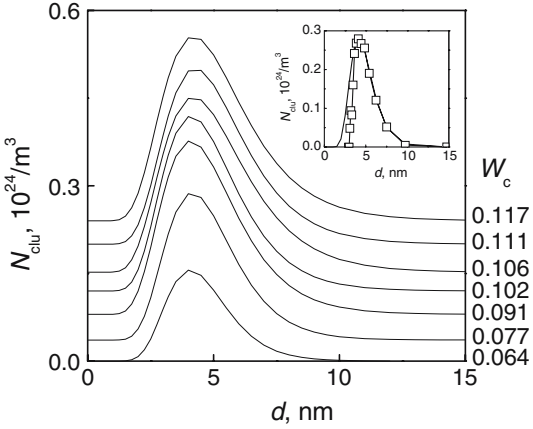

Fig. 4. Fitted CSD for various water content. Each data point is shifted by 0.04 along the ordinate. Inset shows the fit of a log normal distribution function.

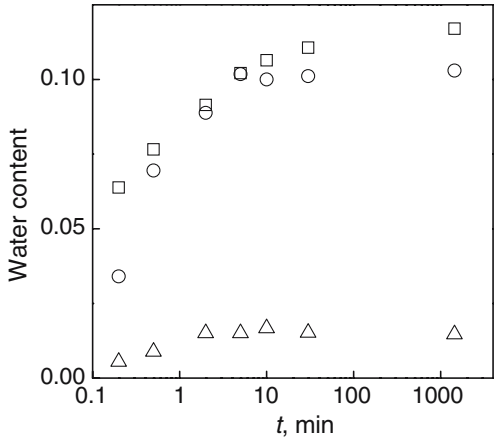

Fig. 5. Three kinds of water content plotted as a function of the soaking time for Nafion with absorbed water; open squares from mass, open circles from the fitted CSD, and open triangles from non-freezable water.

W_c and the cluster water content. This means that clusters are formed by the aggregation of the hydrophilic terminal. W_c by mass includes the excess water for the cluster water content from the fitted CSD. The results for W_c

are essentially inconsistent with those for cluster water content. This excess water is due to the channel water between clusters not included in the clusters of water. We can estimate the channel structure from this excess water.

3.4. Nanostructure of Water Clusters in Nafion with Absorbed Water

We assume that the water clusters in Nafion with absorbed water form a simple cubic lattice. The simple cubic lattice of the water clusters is a good model for the nanostructure that consists of clusters and channels. In this model one cluster has three channels. Based on this simple cubic lattice model, we can estimate the channel length L_{ch} (not including the cluster diameter) and channel cross section S_{ch} of the channel between the water clusters using the following equations:

$$L_{ch} = \frac{1}{3} \times \left(\sqrt[3]{\frac{1}{N_{clu}}} - d \right) \quad \text{and} \tag{4}$$

$$S_{ch} = \frac{W_{up} - W_{log}}{\rho_w N_{clu} V_{Naf} L_{ch}}, \tag{5}$$

where W_{log} is the total water mass in the cluster estimated by the integral of the CSD.

Figure 6 shows L_{ch} and S_{ch} through the water uptake process. In early stages L_{ch} and S_{ch} decrease with increasing soaking time. In later stages L_{ch} holds constant and S_{ch} increases. Water molecules disperse initially in Nafion by diffusion. After that, water clusters are formed by the aggregation of the terminal sulfonic acid groups with hydrophilicity. In the early stages the estimated channel structures may not reflect the actual ones, because there are many dispersed water molecules in Nafion and Nafion and water are in a nonequilibrium state. In later stages cluster formation is completed with the water-saturated clusters. Then the length L_{ch} becomes constant. The cross section S_{ch} increases by the supplied water molecules with an increase of W_c. The cross section S_{ch} shows good agreement with the results of streaming potential data [2,10,11]. Our simple cubic lattice model is a good assumption for the channel structures in Nafion with absorbed water.

3.5. Nanostructural Change of Clusters and Channels by Thermal Degradation

The fitted CSD of water uptake for Nafion aged at 25, 150, and 300°C is shown in Fig. 7. It can be found clearly that the number of

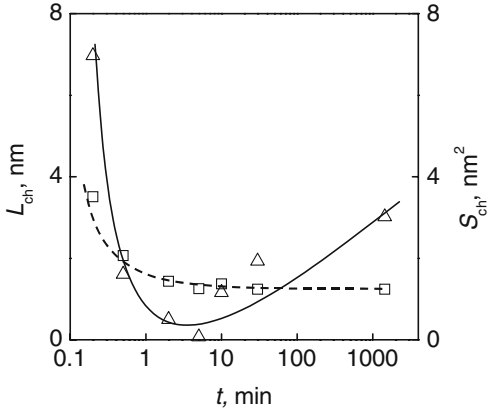

Fig. 6. Channel length L_{ch} (open squares) and channel cross section S_{ch} (open triangles) plotted as a function of the soaking time for Nafion. Solid and dotted curves are guides for the eye.

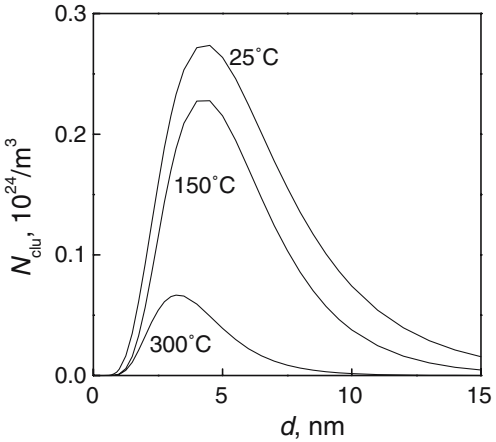

Fig. 7. Fitted CSD for Nafion aged at 25, 150, and 300°C for 1 h.

water clusters N_{clu} decreases in overall diameter range with an increase in the aging temperature. This decrease in the fitted CSD is consistent with the thermal degradation related to SO_2 liberation and the desulfonation in the terminal of the side chain of Nafion [4]. Peak diameters decrease with an increase in the aging temperature.

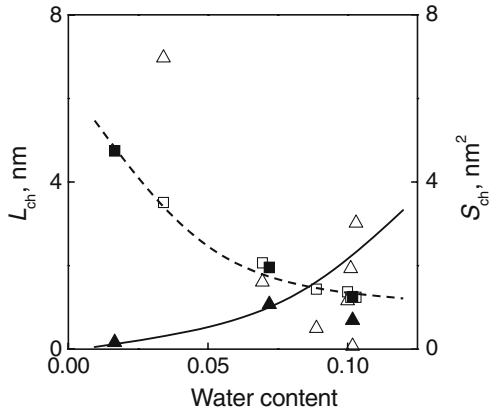

Fig. 8. Channel length L_{ch} (squares) and channel cross section S_{ch} (triangles) plotted as a function of water content for Nafion; open symbols for as received and closed symbols for thermally degraded Nafion. Solid and dotted curves are guides for the eye.

We can also estimate the nanostructure of clusters and channels in thermally degraded Nafion. Figure 8 shows the channel length L_{ch} and channel cross section S_{ch} with various water content for thermally degraded Nafion. Comparison of as received Nafion with thermally degraded Nafion shows that L_{ch} lies on the same curve but S_{ch} differs significantly in the low water content. Through desulfonation, Nafion and water are in an equilibrium state even at the low water content.

The channel cross section S_{ch} would be a dominant factor for a mesh effect in the transport of the protons and ions through Nafion, and the PEFC performance could be improved by control of S_{ch}.

4. CONCLUSION

The CSD for Nafion is obtained from DSC measurements with a stepwise temperature program. The CSD fitted by a log normal distribution function gives useful information for the nanostructure of clusters and channels in Nafion with absorbed water. The fitted CSD for the water absorbed Nafion reveals a peak of approximately 4 nm in diameter. The nanostructure in Nafion with absorbed water consists of at least three kinds of water states, two of which are freezable and non-freezable water in a cluster and another state is the non-freezable water in a channel between the clusters. The non-freezable water within a cluster exists with

a few percent in Nafion with absorbed water. From the assumption of a simple cubic lattice model, we can estimate the channel length L_{ch} between the clusters and the channel cross section S_{ch}. Also, the desulfonation in the terminal of the side chain by thermal degradation causes a change of the nanostructure in Nafion with absorbed water. The channel length L_{ch} decreases monotonically with increasing water content. The channel cross section S_{ch} increases with increasing water content. The nanostructure in Nafion with absorbed water would be an important factor for an improvement in the performance of a PEFC.

REFERENCES

1. T.D. Gierke, G. E. Munn, and F. C. Wilson, *J. Polym. Sci. Phys. Ed.* **19**:1687 (1981).
2. T. Okada, G. Xie, O. Gorseth, S. Kjelstrup, N. Nakamura, and T. Arimura, *Electrochim. Acta* **43**:3741 (1998).
3. S. C. Yeo and A. Eisenberg, *J. Appl. Polym. Sci.* **21**:875 (1977).
4. S. H. de Almeida and Y. Kawano, *J. Therm. Anal. Calorim.* **58**:569 (1999).
5. K. Ishikiriyama, M. Todoki, and K. Motomura,*J. Colloid Interface Sci.* **171**:92 (1995).
6. T. C. Maloney, *User Com 12 of Mettler Toledo* **2** (2000).
7. T. Hironaka, K. Ishikiriyama, Y. Iwato, E. Hayasi, and H. Katagiri, *The TRC News* **78** (Jan. 2002).
8. H. Yoshida and Y. Miura, *J. Membrane Sci.* **68**:1 (1992).
9. C. Yang, S. Srinivasan, A. B. Bocarsly, S. Tulyani, and J. B. Benziger, *J. Membrane Sci.* **237**:145 (2004).
10. G. Xie and T. Okada, *Denki Kagaku* **64**:718 (1996).
11. G. Xie and T. Okada, *J. Electrochem. Soc.* **142**:3057 (1995).